Open Access Library Journal
2023, Volume 10, e10108
ISSN Online: 2333-9721
ISSN Print: 2333-9705

A Biaxial Bending Study of H-Section Steel Member at the Ultimate State

Mohamad Mansour

Department of Civil Engineering, Taiyuan University of Technology, Taiyuan, China
Email: mansour.mohamad777@gmail.com

How to cite this paper: Mansour, M. (2023) A Biaxial Bending Study of H-Section Steel Member at the Ultimate State. *Open Access Library Journal*, **10**: e10108.
https://doi.org/10.4236/oalib.1110108

Received: April 2, 2023
Accepted: May 7, 2023
Published: May 10, 2023

Abstract

The bidirectional compression bending members exhibit interactions among their strength, stiffness, and plastic deformation capacity in their two principal axis directions. Unfortunately, there is limited research on the performance of H-shaped cross-section steel members under bidirectional compression bending controlled by local instability, making it imperative to develop further research in this area. To address this issue, a finite element model was established to investigate the nonlinear performance of H-shaped cross-section members under three combinations of different width-to-thickness ratios. The study aimed to explore the basic mechanical characteristics of bidirectional compression bending of H-shaped members while analyzing the two failure modes caused by different width-thickness ratios. To determine the limit state of H-section steel members under bidirectional compression bending, the energy inflection point method was proposed based on the principle of energy conservation. Additionally, the analysis of the mean stress development of the member section indicates that the limit state of the member determined by this method is reasonable.

Subject Areas

Civil Engineering

Keywords

Ultimate State, h-Section, Steel Member, Biaxial Bending

1. Introduction

The impact of earthquakes on building structures is complex, and studying the performance of components under bidirectional compression and bending is crucial to comprehensively understanding the seismic behavior of structural

components [1]. In bidirectional compression-bending members, when yielding or buckling occurs in one principal axis direction, it diminishes the strength and stiffness of the other principal axis direction simultaneously. There exists an interaction among the strength, stiffness, and plastic deformation capacity in both principal axis directions. These interactions become more significant as the deformation increases, leading to an amplified structural response [2]. The current codes used to calculate the two-way compression bending capacity do not fully consider the interplay between the axial force and the two-way bending moment, leading to limitations [3]. To differentiate the plastic deformation capacity of components, [4] categorizes the sections of flexural and compressive members into four types: I, II, III, and IV. However, the research on H-shaped cross-section bidirectional compression-bending members has primarily focused on type I and type IV cross-section members, with relatively limited research on type II and type III cross-section members controlled by plastic local instability. For Class I H-shaped cross-section members where local instability is not the primary failure mode [5] compiled a finite element calculation program and found that the eccentricity in the strong axis direction had a significant impact on the ultimate bearing capacity.

When dealing with type IV H-shaped sections, where elastic local instability is the primary failure mode, researchers such as Bradford have used the finite strip method to derive the expression of the elastic buckling stress of the section under bidirectional compression bending. [6] conducted two-way eccentric compression tests and theoretical studies on H-shaped cross-section columns with varying plate width-thickness ratios and eccentricities, showing that the current code's correlation curves of two-way bending moments differ significantly from the actual ones. Consequently, the calculation of the bending capacity is overly cautious [7] [8].

When dealing with thin and flexible sections controlled by local buckling (Type II and Type III sections), the bearing capacity can be improved after edge yielding, but full section plasticity cannot be achieved. Currently, there are no relevant codes or research findings that clearly define the limit state of this type of section under bidirectional compression bending. Determining the ultimate bearing capacity of this section is crucial to solving the bearing capacity of components under arbitrary loads and requires immediate attention.

This study focuses on the nonlinear behavior of bidirectional compression bending of H-shaped cross-section members under different width-to-thickness ratios. The component's limit state is determined using the energy inflection point method, and the limit correlation curve of the component under bidirectional compression bending is established.

2. Characteristics

The H-shaped members under bidirectional compression bending exhibit several characteristics. Firstly, when the load is applied, deflection and torsion angle

in two directions appear in the bidirectional compression-bending member, which leads to extreme point instability in the elastic-plastic state. Secondly, the section at the bottom of the column is affected by six reaction forces, including axial force, shear force, bending moments, and second-order torque. Thirdly, the H-shaped section has a large difference in the bending stiffness of the two main axes, which results in the directions of the resultant force and the resultant displacement not coinciding during bidirectional loading. Fourthly, in the elastic stage, the second-order bending moment and torque effect are not obvious, and the directions of the resultant force and the resultant displacement remain unchanged. Fifthly, in the plastic or buckling state, the relationship between the resultant force and the resultant displacement is nonlinear, and the direction of the two changes continuously with the loading. This nonlinear response is one of the important characteristics of the component space.

3. Determination of Limit State

3.1. Determination Method

The determination of the ultimate bearing capacity of a component is essential in engineering design as it directly reflects its resistance and bidirectional compression-bending performance. For H-shaped steel members under uniaxial compression bending, their bending moment-angle ($M-\theta$) curve indicates their bearing capacity, with the inflection point moment on the $M-\theta$ curve being considered as the ultimate bearing capacity moment of the member. These members can reach their limited state of bearing capacity due to local plate buckling or entering full-section plasticity. The inflection point on the moment-angle curve is significant both theoretically and practically.

However, in bidirectional bending, the conventional method of defining the limit state based solely on Mx and My peak values is not applicable since the strong-axis and weak-axis bending moments may not reach their peak values simultaneously. Therefore, some scholars propose analyzing component bearing capacity from an energy perspective, considering the principle of energy conservation in the stability of steel structures as the equilibrium point between the strain energy stored in the system and the work done by the external force.

The energy method utilizes the work Δ2W and the second derivative of the work Δ2W to classify the state of the column member as stable, critical, or unstable. The formula for the second derivative of the work (Δ2W) is provided as:

$$\Delta 2W=\left(\Delta 2Vx+\Delta 2Vy+\Delta 2Vz-2\left(\Delta ux\Delta Vx+\Delta uy\Delta Vy+\Delta uz\Delta Vz\right)\right)\Big/\beta^2 \quad (1)$$

where Δ2Vx, Δ2Vy, Δ2Vz are the increments of the restoring force at the loading end of the column top, respectively, and Δux, Δuy, Δuz are the displacement increments of the loading end of the column top, respectively. β is the restoring force increment and the displacement increment at the loading end of the column top vector angle.

Based on the second derivative of the work, the state of the column member is

classified as stable, critical, or unstable. If Δ2W > 0, the column member is in a stable state. If Δ2W = 0, the column member is in a critical state, and the bearing capacity of the member is at its peak value. If Δ2W < 0, the column member is in an unstable state, and the bearing capacity of the member has already exceeded the peak value.

3.2. Determination of the Lower Limit State of H-Shaped Members under Bidirectional Compression Bending

This section of the paper explains how the authors determined the lower limit state of H-shaped members under bidirectional compression bending. They conducted a two-way compression-bending test on an H-shaped cantilever steel member with the loading end loaded linearly according to the displacement ratio $ux/uy = \tan\alpha$. As the axial deformation of the member is small under two-way bending, the work done by the axial force in the axial direction can be ignored [9].

However, after the member enters the plastic or buckling state, the vector angle β between the resultant force V and the resultant displacement u changes continuously with the loading process. This makes it challenging to obtain the work done by the external force directly using the relevant formula. To overcome this, the authors refer to a loading scheme adopted in literature [10] and obtain the external force work through coordinate transformation [11] [12].

The method involves establishing an original coordinate system x-y with the main axis direction of the component as the coordinate system direction and determining the direction of displacement loading on the original coordinate system. Then, the authors calculate the component forces Vx and Vy of the resultant force in the direction of the main axis of the component and transform them to a new coordinate system X-Y. The new coordinate system is established with the direction of displacement loading in the original coordinate system x-y as the X-axis and the direction perpendicular to the displacement loading as the Y-axis.

The authors explain that the moment of the zero crossing point of the external force Δ2W is the moment of the maximum value of the force VX in the VX-u curve, which is the moment of the energy inflection point. Using this information, they determine the lower limit state of the H-shaped member under bidirectional compression bending. The formula for the resultant force in the displacement direction of the member after transforming Vx and Vy to the new coordinate system X-Y is:

$$VY' = Vx * \sin\alpha + Vy * \cos\alpha \tag{2}$$

where VY' is the resultant force in the displacement direction, Vx and Vy are the component forces of the resultant force in the direction of the main axis of the component, and α is the angle between the direction of displacement loading and the main axis direction of the component.

4. Finite Element Model

The complex behavior of H-shaped double-curved members under plastic de-

formation poses a challenge in obtaining explicit expressions, hence requiring the use of finite element software and mechanism analysis to examine their performance. In order to investigate the bidirectional compressive and bending behavior of H-shaped steel members, a bidirectional loading analysis was conducted on three groups of H-shaped cantilever members with varying aspect ratios and an axial compression ratio of 0.2. By comparing the results, the impact of local buckling and loading path on bidirectional compressive and bending performance can be evaluated. The H-shaped section's dimensions are specified in Table 1 displays the basic parameters of the three members. The members are named R-n-rw-rf, where R represents bidirectional compressive and bending, r_w and r_f denote the ratio of the width to thickness of the web and flange, respectively, and $n = N/(Afy)$ is the axial compression ratio of the section. The cantilever member model was set at a height of L = 1500 mm, which is roughly half the height of a typical residential floor. The yield bending moments considering the effect of axial compression are denoted as Mecx and Mecy.

To simulate the nonlinear behavior of H-shaped double-curved members under bidirectional compressive and bending, ABAQUS, a general-purpose software, was used. The modeling was done using S4R elements, and the steel material was represented by an ideal elastic-plastic model, where the yield strength fy was 345 MPa, the elastic modulus E was 2.06 × 105 MPa, and the Poisson's ratio was 0.3. The column was loaded from the top, first with a constant axial compression force and then with horizontal displacement along both principal axes at the top to achieve uy/ux = tanα. Loading analyses were carried out with α = 0˚, 15˚, 30˚, 45˚, 60˚, 75˚, and 90˚, which correspond to unidirectional loading along the x-axis (bending around the weaker axis direction) and y-axis (bending around the stronger axis direction), respectively. The finite element model of H-shaped cantilever members in references [13] was referenced during the modeling process.

5. Analysis of Finite Element Results Units

5.1. Analysis of Failure Mechanism

The findings from the finite element simulations reveal that the failure of all the components was attributed to the buckling of the bottom plate. However, based on the distinctive plastic development of the component section, the failure can be categorized into two types: buckling failure dominated by local buckling, such

Table 1. Modeling process.

Member	Loading direction	rw	rf	n	Maximum load (kN)	Maximum bending moment (kNm)
R-0.2-25-7	x-axis-y-axis	25	7	0.2	255	49.3
R-0.2-55-14	x-axis-y-axis	55	14	0.2	139	25.3
R-0.2-85-19	x-axis-y-axis	85	19	0.2	103	19.2

as in components R-0.2-85-19 and R-0.2-55-14, and non-buckling failure, where the section had entered full-section plasticity, as observed in component R-0.2-25-7. This section focuses on the analysis of the average stress and bending moment development in the two principal axis directions during the $\theta/\theta e \leq 5$ stages for models R-0.2-25-7 and R-0.2-85-19 under loading conditions of $\alpha = 30^{\circ}$. The yield rotation angle θe is also considered. The aim of this analysis is to investigate the plasticity and buckling failure mechanisms of the components subjected to bidirectional compression-bending. The average stress is explained in reference [14]. The results of the calculations for typical components are illustrated in Figure 1.

The destruction modes of components at $\theta/\theta e = 5$ are displayed in Figure 1(a) and Figure 1(b). For component R-0.2-25-7, which has a small wing-web width-thickness ratio, the plate remains flat and uniformly colored with no occurrence of local buckling, indicating it is in the stage of plastic deformation without local buckling. However, for component R-0.2-85-19, which has a large wing-web width-thickness ratio, both the wing and web experience significant buckling deformation, with uneven color distribution, indicating it is in the stage

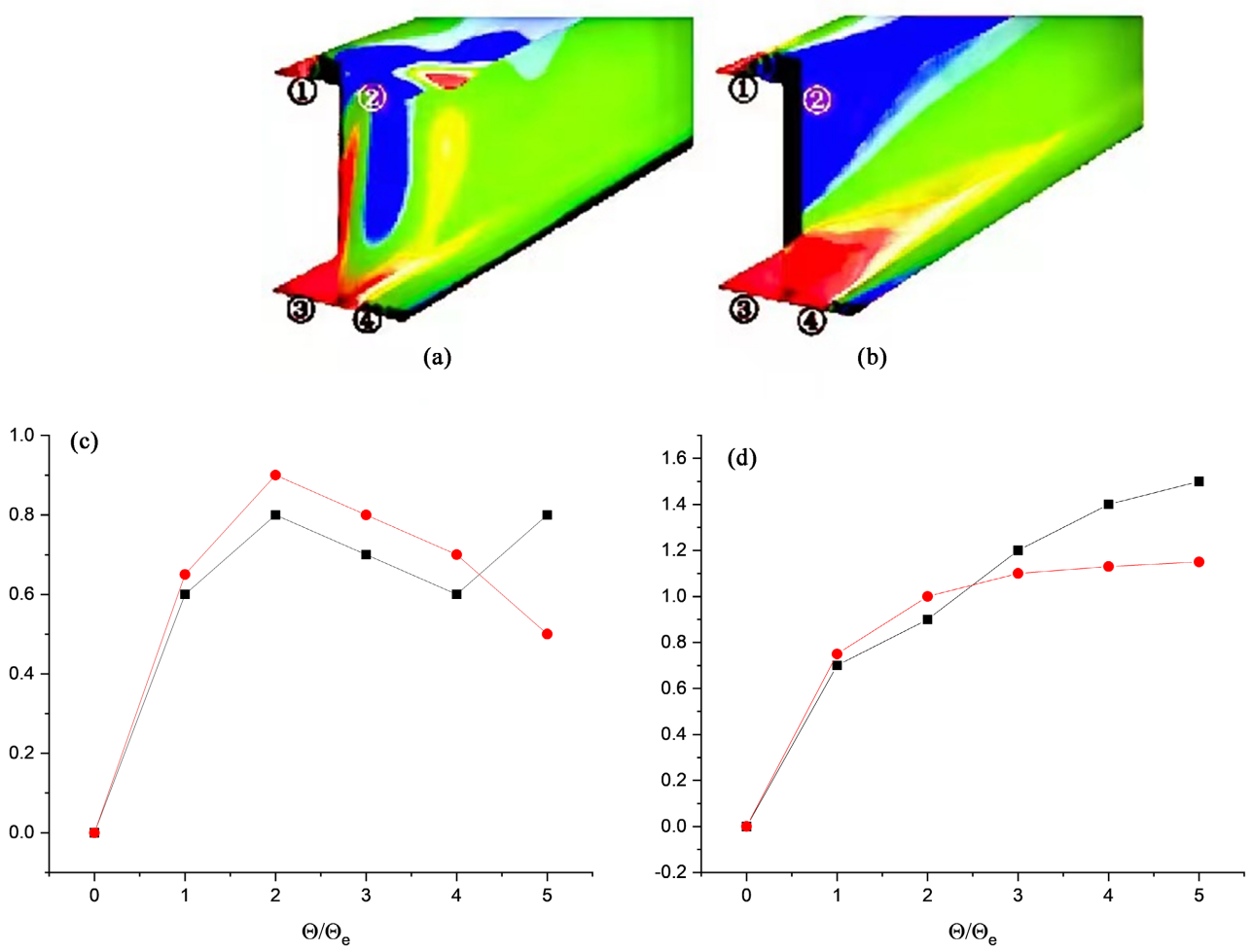

Figure 1. (a) R-0.2-85-19DF; (b) R-0.2-25-7DF; (c) R-0.2-85-19BBM; (d) R-0.2-25-7BBM.

of local buckling development. This shows that the width-thickness ratio of the plate has a significant influence on the destruction mode of the component under the same loading conditions.

The plastic development process of the components can be traced by tracking the stress development within the range of $\theta/\theta e = 5$. For component B-0.2-25-7, as there is no occurrence of local buckling, plastic stress continues to develop in the original equilibrium configuration with the order of development being wing 2, wing 3, wing 1, and wing 4, while the stress in the web continually increases. However, for component R-0.2-97-19, the stress at the outer edge of wing 2 degenerates to 0 after $\theta/\theta e = 2$, indicating that wing 2 buckles at around $\theta/\theta e = 2$, leading to buckling deformation of wing 1 and web. Although wings 3 and 4 are still in an unbuckled state, the stress of each plate no longer increases to satisfy the balance condition of the cross-section. The fundamental difference between the stress development process of buckled and unbuckled cross-sections reveals the corresponding relationship between the width-thickness ratio of the plate and the stress development process under biaxial bending conditions.

Biaxial bending moment is the macroscopic and quantitative manifestation of the stress development process of the cross-section. The two principal axis bending moments Mx and My at the bottom section of each component are extracted and non-dimensionalized using the corresponding uniaxial bending yield moments Mecx and Mecy. The chord displacement u at the top of the column is also extracted, and the chord rotation angle θ is obtained, which is then non-dimensionalized using the yield rotation angle θe and plotted in **Figure 1(c)** and **Figure 1(d)**. The My bending moment of the component is mainly contributed by the stress gradient of the left and right wings, while the Mx bending moment is mainly contributed by the stress gradient of the upper and lower wings and web. For component R-0.2-25-7, when θ/θ e = 2, wing 2 reaches full plasticity, and the stress in the left and right wings can no longer develop in different directions, so My reaches its peak value. However, the other wings and web are still in an elastic or partially plastic state, so as plastic deformation deepens, the bending stiffness in the strong axis direction begins to decrease, but Mx still continues to increase. For component R-0.2-85-19, when the plate buckles at around $\theta/\theta e = 2$, the average stress in the buckled plate decreases. To maintain cross-sectional force balance, wings 3 and 4 cannot develop incremental stress even though they have not buckled, so Mx and My both reach their peak values simultaneously. It should be noted that the buckled wing of component R-0.2-85-19 is divided into two sections according to the stress distribution, namely, the edge-bulging section and the near.

5.2. Limit State Analysis of Components

The limit state of an H-shaped steel member under biaxial compression and bending is determined using the method of energy inflection point. Three models are extracted to analyze the stress and biaxial bending moment development

of the cross-section under biaxial loading directions of 15˚, 30˚, 45˚, 60˚, and 75˚ with $\theta/\theta e \leq 5$.

As analyzed in section 5.1, the failure mechanism of the H-shaped steel member is due to the early local buckling of the plate or excessive plastic deformation of the member. The moment when the plate buckles and the moment of maximum plastic deformation of the cross-section correspond to the moment of maximum average stress of the member, which is the basic characteristic of the limit state.

For the B-0.2-25-7 member, no plate buckling occurs before reaching the limit state, and at the limit moment for each biaxial loading direction, the enveloped tensile and compressive stress area is the largest and most stable, indicating that the cross-section's average stress has reached its maximum. At the limit moment, the bending moment Mx around the strong axis of the member increases slowly in the 15˚ and 30˚ loading directions, while in the 45˚, 60˚, and 75˚ loading directions, it is at its maximum and remains stable. The bending moment My around the weak axis is stable in the 15˚ loading direction but decreases in the 30˚, 45˚, 60˚, and 75˚ loading directions.

For the R-0.2-55-14 and R-0.2-85-19 members, local instability failure dominated by plate buckling occurs. The R-0.2-55-14 member is selected for limit state analysis. The corresponding moments at the limit state in the 15˚, 30˚, 45˚, 60˚, and 75˚ loading directions are $\theta/\theta e = 3.3$, $\theta/\theta e = 3.3$, $\theta/\theta e = 2.7$, $\theta/\theta e = 2.1$, and $\theta/\theta e = 1.7$, respectively. By tracking the stress development of the member, it can be seen that the average stress reaches its maximum at this time, and the plate begins to buckle at the outer edge of flange 2 in the next moment, leading to a reduction in the cross-section's average stress development zone. At the limit moment for each loading direction, the bending moment Mx around the strong axis of the member increases slowly in the 15˚ and 30˚ loading directions, while in the 45˚, 60˚, and 75˚ loading directions, it is at its maximum. The bending moment My around the weak axis is at its maximum in the 15˚ loading direction, but begins to decrease gradually due to the buckling of the flange edge in the next moment and is in the decreasing phase in the 30˚, 45˚, 60˚, and 75˚ loading directions, close to the uniaxial limit value. The R-0.2-85-19 member follows the same development pattern as the R-0.2-55-14 member, but because of its larger plate width-to-thickness ratio, it reaches the limit moment earlier.

5.3. Bending Moment Correlation

That involves plotting Mx-My correlation curves to obtain ultimate state correlation curves, which are important for bi-directional compression-bending design. The authors place the two principal axis bending moments under different directional angles in the same graph to obtain the Mx-My correlation curves.

The ultimate state correlation curve and the envelope of the two principal axis bending moments are separately plotted in **Figure 2** for each component's bi-directional bending moment correlation curves. **Figure 2** provides a summary

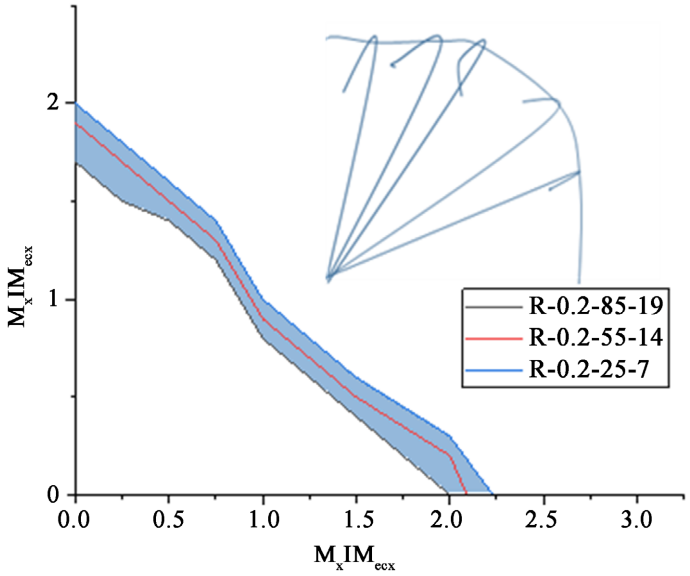

Figure 2. Limit state analysis of components.

of the ultimate correlation curves for the three component models. The results show that the two principal axis correlation curves of the three calculated components gradually decrease with an increase in the aspect ratio of the plate, but the correlation curves have a similar shape.

In summary, the study involves plotting Mx-My correlation curves to obtain ultimate state correlation curves, which are essential for bi-directional compression-bending design. The results show that the two principal axis correlation curves of the three calculated components gradually decrease with an increase in the aspect ratio of the plate, but the correlation curves have a similar shape. **Figure 2** summarizes the ultimate correlation curves of the three component models, providing a valuable reference for designing bi-directional compression-bending structures.

6. Conclusions

The article proposes a new approach for determining the ultimate limit state of H-section steel members under biaxial bending, which involves identifying the energy inflection point. The authors investigate the nonlinear behavior of H-section members under biaxial bending for three different width-to-thickness ratios and various directions of load angles.

For flexible members controlled by local buckling, the buckled flange's edge section exits the work, while the flange section near the web maintains a certain stress due to the web's constraint, which can be considered as the effective width. Consequently, even after buckling, the two primary axes can still maintain a certain bending resistance.

The ultimate limit state stress obtained by the energy inflection point method exhibits the most complete stress development, which can be regarded as the moment of plate buckling or the maximum moment of cross-sectional plastic

development. However, under biaxial bending, the uniaxial bending moments Mx and My do not reach their respective ultimate limit states simultaneously, and the average stress development of each corresponding ultimate limit state is not the maximum moment. Therefore, it is not reasonable to determine the ultimate limit state of biaxial bending of the member by the ultimate limit state of uniaxial bending.

The nonlinear behavior of H-section steel members under biaxial bending is influenced by various factors, making it necessary to obtain a practical and reasonable design method for H-section steel members under biaxial bending. The proposed method can be applied to design H-section steel members subjected to biaxial bending with different load angles and width-to-thickness ratios.

Conflicts of Interest

The author declares no conflicts of interest.

References

[1] Yue, Y., Chen, T., Bai, Y., Lu, X., Wang, Y. and Musanyufu, J. (2019) Seismic Design and Analysis of Reinforced Concrete Buckling-Restrained Braced Frame Buildings with Multi-Performance Criteria. *International Journal of Distributed Sensor Networks*, **15**. https://doi.org/10.1177/1550147719881355

[2] Zheng, Y., Yang, S. and Lai, P. (2020) Hysteretic Behavior of Multi-Cell L-Shaped Concrete-Filled Steel Tubular Columns at Different Loading Angles. *Engineering Structures*, **202**, Article No. 109887. https://doi.org/10.1016/j.engstruct.2019.109887

[3] Li, S., Guo, C., Hao, L., Kang, Y. and An, Y. (2019) *In-Situ* EBSD Study of Deformation Behaviour of 600 MPa Grade Dual Phase Steel during Uniaxial Tensile Tests. *Materials Science and Engineering*: *A*, **759**, 624-632. https://doi.org/10.1016/j.msea.2019.05.083

[4] Cheng, X., Chen, Y. and Pan, L. (2013) Experimental Study on Steel Beam-Columns Composed of Slender H-Sections under Cyclic Bending. *Journal of Constructional Steel Research*, **88**, 279-288. https://doi.org/10.1016/j.jcsr.2013.05.020

[5] Zhang, Z., Xu, S., Nie, B., Li, R. and Xing, Z. (2020) Experimental and Numerical Investigation of Corroded Steel Columns Subjected to in-Plane Compression and Bending. *Thin-Walled Structures*, **151**, Article No. 106735. https://doi.org/10.1016/j.tws.2020.106735

[6] Landi, L., Stecconi, A., Morettini, G. and Cianetti, F. (2021) Analytical Procedure for the Optimization of Plastic Gear Tooth Root. *Mechanism and Machine Theory*, **166**, Article No. 104496. https://doi.org/10.1016/j.mechmachtheory.2021.104496

[7] Cheng, X., Wang, X., Zhang, C. and Duan, D. (2021) Study on Ultimate Capacity of Steel H-Section Members under Combined Biaxial Bending and Axial Force. *International Journal of Steel Structures*, **21**, 1804-1822. https://doi.org/10.1007/s13296-021-00536-4

[8] Khabaz, A. (2015) 2D Investigation of Bonding Forces of Straight Steel Fiber in Concrete. *Open Access Library Journal*, **2**, e1991. https://doi.org/10.4236/oalib.1101991

[9] Jia, L., Zhao, Y., Liu, H., Chen, Z. and Kashan, K. (2022) Flexural Performance of Weld-Strengthened Steel Beam-Square Column Joints Subjected to Axial Column

Loading. *Journal of Constructional Steel Research*, **199**, Article No. 107599. https://doi.org/10.1016/j.jcsr.2022.107599

[10] Shen, Z., Liu, B., Cheng, X. and Zhou, G. (2023) Stressing State Features of H-Steel Columns under Cyclic Biaxial Bending Action Revealed from Experimental Residual Strains. *Case Studies in Construction Materials*, **18**, e01518. https://doi.org/10.1016/j.cscm.2022.e01518

[11] Gang, W. and Caiqi, Z. (2021, October) Experimental and Theoretical Study on the Bearing Capacity of FGC Joints for Single-Layer Aluminium Alloy Lattice Shell Structures. *Structures*, **33**, 2445-2458. https://doi.org/10.1016/j.istruc.2021.05.067

[12] Tan, Y., Li, X., Zhang, Q., Zhang, S., Li, Z. and Qiu, L. (2023) Mechanical Performance of an Improved Aluminium Alloy Gusset Joint under Simplex and Complex Load States. *Thin-Walled Structures*, **186**, Article No. 110703. https://doi.org/10.1016/j.tws.2023.110703

[13] Cheng, X. and Chen, Y. (2018) Ultimate Strength of H-Sections under Combined Compression and Uniaxial Bending Considering Plate Interaction. *Journal of Constructional Steel Research*, **143**, 196-207. https://doi.org/10.1016/j.jcsr.2017.12.019

[14] Zhang, X., Li, J., Yu, Z., Yu, Y. and Wang, H. (2017) Compressive Failure Mechanism and Buckling Analysis of the Graded Hierarchical Bamboo Structure. *Journal of Materials Science*, **52**, 6999-7007. https://doi.org/10.1007/s10853-017-0933-9